

## Chapter 10

### Adjacent seas of the Pacific Ocean

Although the adjacent seas of the Pacific Ocean do not impact much on the hydrography of the oceanic basins, they cover a substantial part of its area and deserve separate discussion. All are located along the western rim of the Pacific Ocean. From the point of view of the global oceanic circulation, the most important adjacent sea is the region on either side of the equator between the islands of the Indonesian archipelago. This region is the only mediterranean sea of the Pacific Ocean and is called the Australasian Mediterranean Sea. Its influence on the hydrography of the world ocean is far greater in the Indian than in the Pacific Ocean, and a detailed discussion of this important sea is therefore postponed to Chapter 13. The remaining adjacent seas can be grouped into deep basins with and without large shelf areas, and shallow seas that form part of the continental shelf. The Japan, Coral and Tasman Seas are deep basins without large shelf areas. The circulation and hydrography of the Coral and Tasman Seas are closely related to the situation in the western South Pacific Ocean and were already covered in the last two chapters; so only the Japan Sea will be discussed here. The Bering Sea, the Sea of Okhotsk, and the South China Sea are also deep basins but include large shelf areas as well. The East China Sea and Yellow Sea are shallow, forming part of the continental shelf of Asia. Other continental shelf seas belonging to the Pacific Ocean are the Gulf of Thailand and the Java Sea in South-East Asia and the Timor and Arafura Seas with the Gulf of Carpentaria on the Australian shelf.

### The Bering Sea and the Sea of Okhotsk

The two seas at the northern rim of the Pacific Ocean are characterized by subpolar conditions. Both are surrounded by land masses on three sides and separated from the main ocean basins by island arcs with deep passages, allowing entry of Pacific Deep Water. Another feature these two marginal seas have in common is their nearly equal division into deep basins and regions belonging to the continental shelf or rise. The *Bering Sea* is set between the Siberian and Alaskan coasts and approximates the shape of a sector with a radius of 1500 km, the circular perimeter being described by the Alaska Peninsula and the Aleutian Islands. It is the third largest marginal sea (after the Arctic and Eurafrian Mediterranean Seas), with a total area of  $2.3 \cdot 10^6$  km<sup>2</sup> and a total volume of  $3.7 \cdot 10^6$  km<sup>3</sup>. Northwest of a line from the Aleutian islands near 166°W to the Siberian coast near 179°E the Bering Sea is shallower than 200 m and forms part of the vast Siberian-Alaskan shelf which continues through Bering Strait into the Chukchi Sea. Southeast of that line depths fall off rapidly, reaching 3800 - 3900 m over most of the region. The Shirshov Ridge runs along 171°E with depths between 500 m and 1000 m. The slightly shallower Bowers Ridge forms a submarine arc from the Aleutian islands along 180° and then 55°N. Together, these ridges divide the western Bering Sea into three basins (Figures 10.1 and 8.3).

Knowledge of the circulation in the Bering Sea is still incomplete, and circulation schemes proposed by different authors show considerable variation. With one exception near 180°, sill depths between the Aleutian islands east of 171°E are generally less than 1000 m, and although tidal currents between the islands are strong -  $1.5$  m s<sup>-1</sup> are common, and  $4$  m s<sup>-1</sup> have been reported - net transport through most passages appears to



Currents in the shallow eastern Bering Sea draw on the surface waters of the Alaskan Stream only and therefore receive their inflow through a shallow but broad passage at 165°W. Observed speeds in the passage are about  $0.1 \text{ m s}^{-1}$ , while over most of the shelf long-term mean velocities do not exceed  $0.03 \text{ m s}^{-1}$ . For reasons related to coastal and shelf dynamics - a topic outside the scope of this text - they are coupled with a system of fronts, along which most of the transport occurs. They are also strongly influenced by the local winds and therefore strongest in August and September when the Bering Sea is ice-free. (Ice begins to form in river mouths during October. In early November sea ice is found south of Bering Strait, and by January ice covers the entire shelf. Ice coverage during this time is usually 80 - 90%. Off Kamchatka the inflow of very cold air from Siberia results in ice coverage well beyond the shelf. Disintegration of the ice sheet starts in April and continues into July, when the Bering Sea is again free of ice.)

Currents in the northernmost section of the Bering Sea are relatively strong despite shallow water depths, being driven by sea level differences across Bering Strait. Flow through the 45 m deep Bering Strait varies between  $0.1 \text{ m s}^{-1}$  in summer and  $0.5 \text{ m s}^{-1}$  in winter. Most of its water is supplied by the Anadyr Current which flows at about  $0.3 \text{ m s}^{-1}$  and varies little with season. To compensate for the seasonal difference, flow through Shpanberg Strait is northward in winter but reverses to weakly southward in summer (Muench *et al.*, 1988).

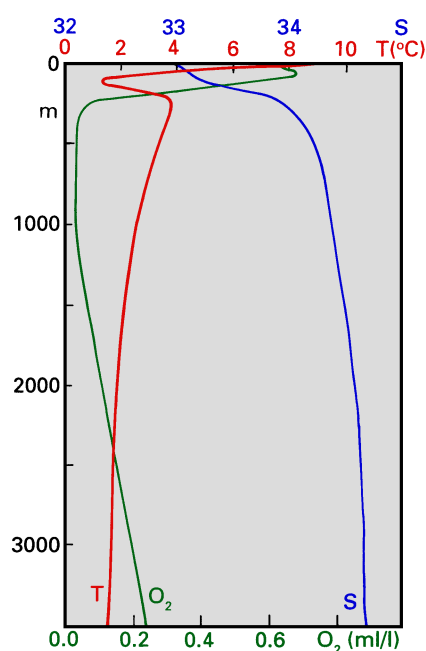


Fig. 10.2. Temperature  $T$  ( $^{\circ}\text{C}$ ), salinity  $S$ , and oxygen  $O_2$  (ml/l) as functions of depth in the Bering Sea, at a station near the centre of the western gyre ( $57^{\circ}\text{N}$ ,  $167^{\circ}\text{E}$ ).

The water mass structure is controlled by advection of water from the Pacific Ocean proper and modification of water properties on the shelf. Station data show a pronounced temperature minimum at or below 100 m depth, a rapid rise of salinity within the upper 300 m from low surface values, and generally low oxygen concentration (Figure 10.2). They indicate the presence of three water masses. The water above the temperature



of the Bering Sea, the main division being along the 1000 m isobath which runs diagonally through the sea from south of the Kamchatka Peninsula toward northwest (Figures 10.3 and 8.3). To the northeast of this line the depth gradually shallows to 500 m in the vicinity of 54°N and to 200 m near 57°N, although departures from this rule occur

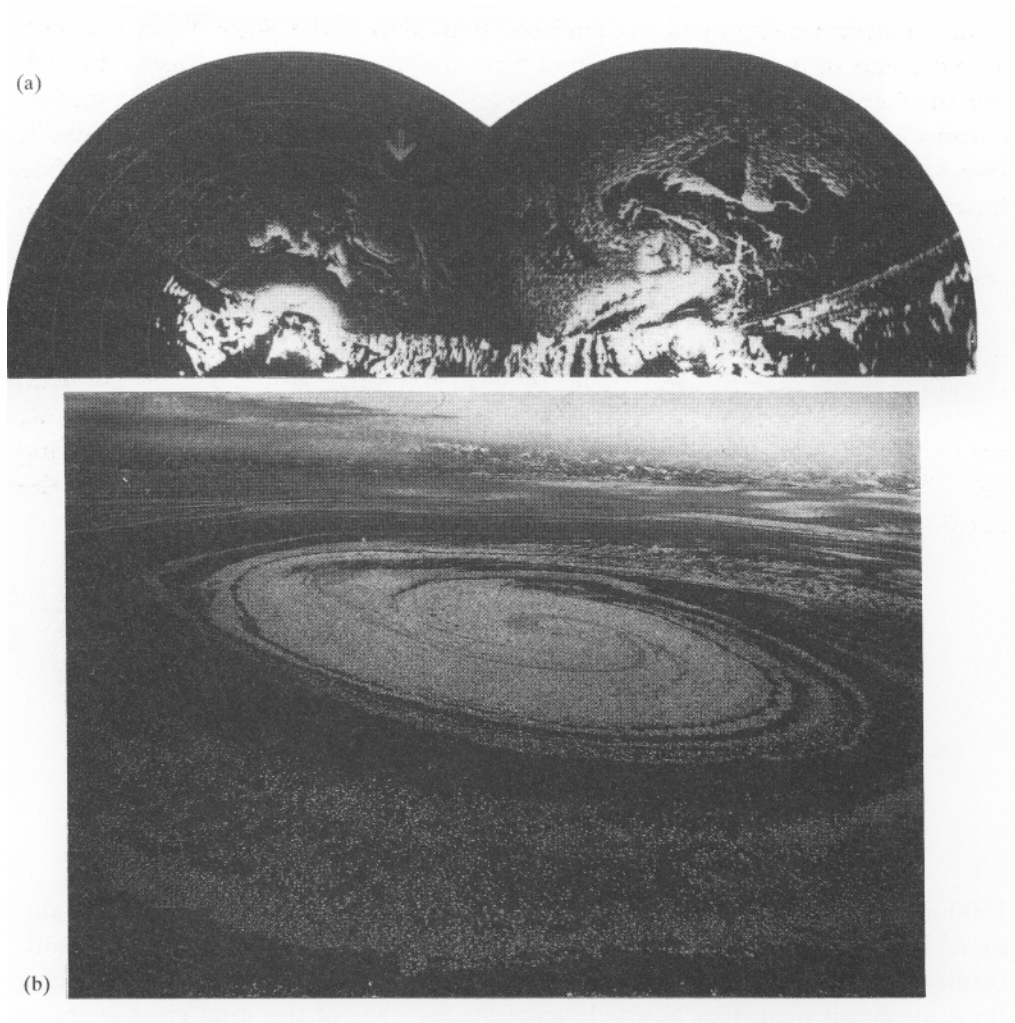


Fig. 10.4. Eddies spawned by the Soya Warm Current. (a) A composite of two radar images obtained at two coastal stations on Hokkaido; (b) a photograph of the eddy marked by the arrow in a) taken from an aircraft at 3500 m altitude. In both figures the eddies are made visible by ice belts composed of uniform ice floes with about 10 m diameter. The diameter of the eddy in (b) is about 20 km. From Wakasutchi and Ohshima (1990).



separates the Yamato Basin to the east, which is somewhat deeper than 2500 m, from the Japan Basin to the west which in this part shows a complicated topography with depths of 1000 - 2500 m.

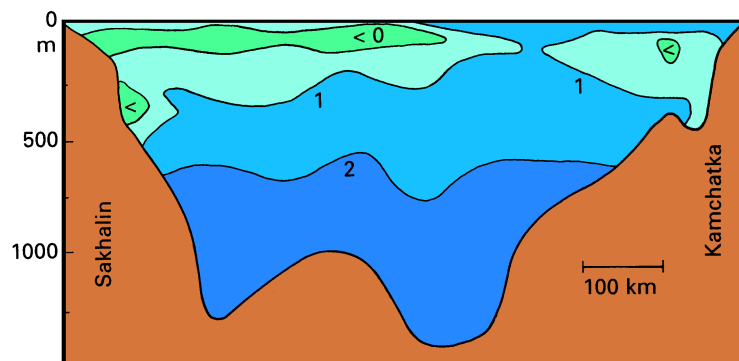


Fig. 10.5. A temperature section (°C) through the southern Okhotsk Sea. Note the lower minimum temperatures in the west, a result of the cyclonic circulation which brings the cold shelf water to the western part first. See Fig. 10.3 for the location of the section.

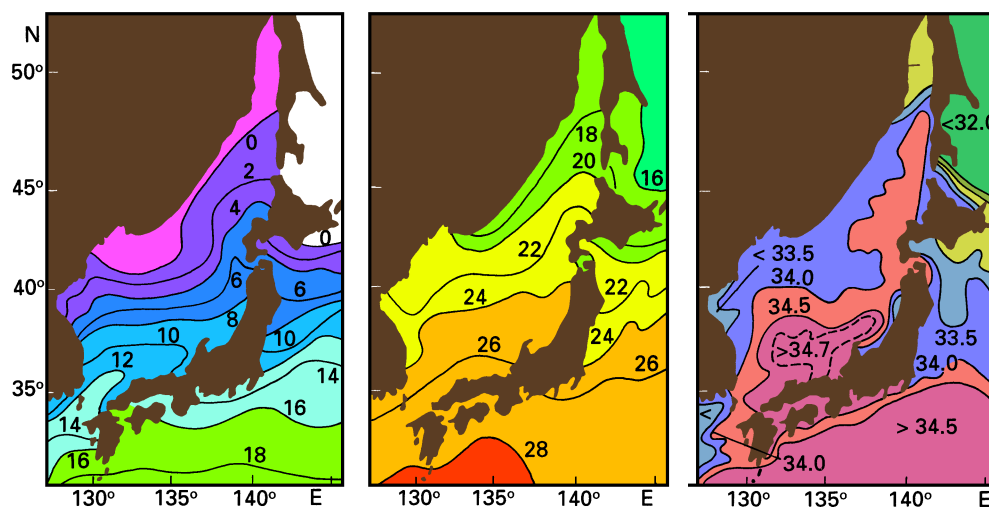


Fig. 10.6. Hydrographic conditions at the surface of the Japan Sea. (a) Temperature (°C) in February, (b) temperature (°C) in August, (c) annual mean salinity.

Given the topographic features of great depth, shallow sills, and restricted communication with the open ocean, the conclusion that the Japan Sea is a mediterranean sea does not seem far-fetched. However, the geographic location at the crossroads between two mighty western boundary currents prevents the establishment of mediterranean characteristics, and the term



Polar Front is found in the Pacific Ocean. The complexity of the region east of Japan, seen in the satellite observations of Figure 8.18, is thus partly the result of the existence of islands in the path of the North Pacific western boundary current which allow water from the Kuroshio to bypass the Oyashio in the west and enter the region from the northwest.

Cold water enters the Japan Sea with the *Liman Current* from the Sea of Okhotsk; some continues southward along the western coast to northern Korea as the *North Korea Cold Current* before it joins the northward flow in the Polar Front. The central part of the Japan Sea is dominated by slow southward cold water movement into the Polar Front; this flow is known as the *Mid-Japan Sea* or *Maritime Province Cold Current*.

The Tsushima Current separates into two branches around the Tsushima Islands which divide Korea Strait near 35°N into a western and an eastern channel. It flows strongest in summer (August) when it carries about 1.3 Sv (about 2% of the total Kuroshio transport) with speeds of up to 0.4 m s<sup>-1</sup> and weakest in winter (January) when its transport amounts to just 0.2 Sv and speeds are below 0.1 m s<sup>-1</sup>. Most of the summer transport passes through the western channel and follows the Korean coast until it separates near 37 - 38°N and follows the Polar Front. Flow through the eastern channel, which is weak throughout the year, follows the Japanese coast closely. Northeastward transport in the central Japan Sea is fairly steady at 2.5 Sv throughout the year; this incorporates the transport of cold water brought in by the North Korea and Mid-Japan Sea Cold Currents.

The separation of the Tsushima Current from the Korean coast is accompanied by instabilities typical for western boundary currents. This includes the formation of large eddies and major shifts in the paths of the two branches. Figure 10.8 shows that in early 1982 the situation depicted schematically in Figure 10.7 was observed. The western branch extends northward as the East Korea Warm Current and establishes the Polar Front north of Ulleung Island (*U* in the Figure). Eddy shedding is evident between Ulleung Island and 35°N. In contrast, during early 1981 the East Korea Warm Current did not proceed beyond 36°N and rejoined the main Tsushima Current along the Japanese coast, producing strong deformations of the Polar Front. This situation was observed to persist for six months.

The seasonal variability of the Tsushima Current is associated with strong seasonal changes of the hydrography. The sea surface salinity in Korea Strait is comparable to open ocean salinities during winter, with values close to 35 (Figure 10.9). These values fall to below 32.5 during summer when the Tsushima Current takes in large amounts of Yellow Sea water which is diluted by river runoff during the Summer Monsoon. The dilution effect does not reach much below 50 m depth and in most areas does not extend down to 30 m. Going north, the annual range of salinity is reduced by mixing; off Hokkaido surface salinity varies between 33.7 and 34.1. Seasonal changes in the Japan Sea also play an important role in the heat transfer between ocean and atmosphere. As Figure 10.6 shows, the sea surface temperature rises by 14 - 18°C from winter to summer, a warming that is almost entirely a result of increased inflow of subtropical Kuroshio water. The heat advected from the tropics is transferred to the atmosphere during winter by cold strong winds from Siberia.

Below the surface water is what is known as the *Japan Sea Middle Water* (again an Asian tradition; elsewhere this water would be called Intermediate Water). It occupies the depth range 25 - 200 m and is characterized by a rapid drop of temperature from 17°C to 2°C. Compared with the major oceans it takes the place of both Central and Intermediate Water; but its depth distribution is much more restricted. The warmer layers of Middle Water are advected into the Japan Sea from the Kuroshio, while the colder layers are formed through a



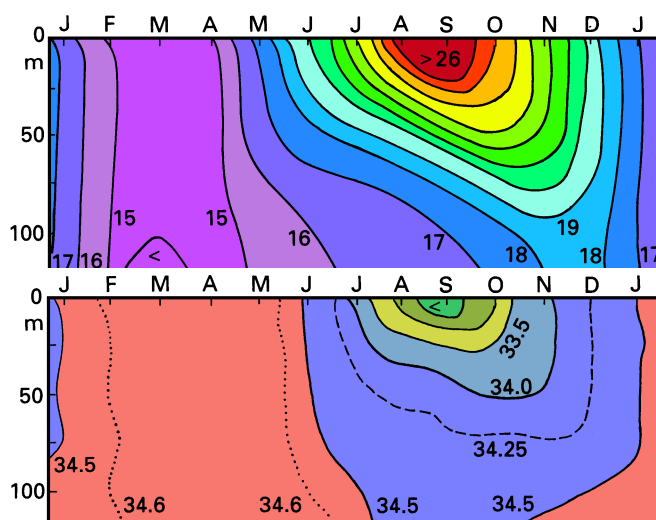


Fig. 10.9. Seasonal variation of the hydrography in Korea Strait. (a) Temperature ( $^{\circ}\text{C}$ ), (b) salinity (full lines use a contour interval of 0.5). From Inue *et al.* (1985)

Japan Sea Deep Water, usually known as *Japan Sea Proper Water*, occupies all depths below 200 m (84% of the volume of the Japan Sea). Its hydrographic properties are remarkably uniform (temperature  $0 - 1^{\circ}\text{C}$ , salinity 34.1), a result of the isolation from all other ocean basins by the shallow sills. The water mass is formed by winter convection north of  $43^{\circ}\text{N}$  and in the region  $41^{\circ} - 42^{\circ}\text{N}$ ,  $132^{\circ} - 134^{\circ}\text{E}$ . Details of the formation process are not well known but it seems likely that salt advection from the Tsushima Current is an important factor, since deep convection will be inhibited by low densities. Instabilities of the Polar Front such as those seen in Figure 10.8 play an important role in transferring salt from the Tsushima Current into the northern regions and may thus influence the rate of formation of Japan Sea Proper Water. Compared to the same depth range in the open North Pacific Ocean, the water in the deep basins of the Japan Sea is extremely well ventilated. Tritium, a product of bomb testing that entered the ocean in vast quantities some 30 years ago, had not yet reached the north Pacific waters below 1000 m depth in 1985 but was present below 2000 m depth in the Japan Sea. Oxygen levels below the thermocline are also much higher in the Japan Sea than in the open North Pacific Ocean, the Sea of Okhotsk, and the Bering Sea which are typically 1 - 2 ml/l (Figure 9.4). Oxygen values in the Japan Sea Proper Water are near 6 ml/l above 2000 m, falling off only slightly to 5.5 ml/l below. The difference in oxygen content below and above the 2000 m level is most likely a reflection of the existence of two formation regions. More recently high quality CTD data have shown a change in the gradient of potential temperature at the same depth (Figure 10.10). Some authors use these observations to differentiate between two variants of Japan Sea Proper Water, which they call Japan Sea Deep Water (200 - 2000 m) and Japan Sea Bottom Water (2000 m - bottom). The consistent temperature difference of  $0.01^{\circ}\text{C}$  between Bottom Water in the



above those of the coastal waters (Figure 10.12). Current speeds are generally below  $0.2 \text{ m s}^{-1}$  and decrease rapidly with depth; water temperatures below the 50 m isobath remain below  $10^\circ\text{C}$  during most of the summer. (This water is known as the Yellow Sea Bottom Cold Water; Figure 10.11.) The *China Coastal Current* brings water of low salinity from the northern Yellow Sea southward. A narrow coastal current along the west coast of Korea brings low salinity water from the Bohai Gulf. The *Taiwan Warm Current* carries water of oceanic properties northward, some of it as an offshoot from the Kuroshio and some through Taiwan Strait. The second path has been well documented for the period of the summer monsoon; but there is some evidence that supply from Taiwan Strait continues through winter. More observations are required to clarify the situation. Further north the path of the Taiwan Warm Current overlaps partly with that of the China Coastal Current, particularly in winter when it flows against the wind and submerges, leaving the upper 5 m of the water column to the southward flowing China Coastal Current, and during all seasons near the mouth of the Yangtze River where it is flooded by diluted water of low density (Figure 10.13).

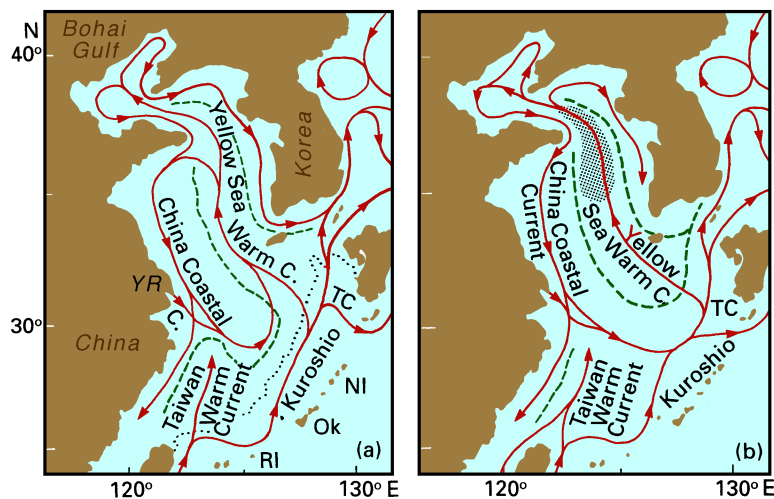


Fig. 10.11. Circulation of the East China and Yellow Seas. (a) During the winter monsoon, (b) during the summer monsoon. TC: Tsushima Current, Ky: Kyushu, NI: Nansei Islands, Ok: Okinawa, RI: Ryukyu Islands, YR: Yangtze River. The shaded area in (b) indicates the region of the Yellow Sea Bottom Cold Water.

The alternating southward and northward flows are separated by frontal regions. The current system exists throughout the year, the Yellow Sea Warm Current heading into the northerly monsoon winds during winter, and the coastal currents opposing the southerly winds of the summer monsoon. Unlike the Yellow Sea Warm Current, which is much weaker when it is opposed by the monsoon winds, the China Coastal Current is strengthened by river runoff from monsoonal rainfall in summer. The current therefore continues unabated against the weak but opposing winds and extends southeastward. Taking



**The South China Sea**

Continuing south in the sequence of marginal seas in the western Pacific Ocean, the South China Sea begins with Taiwan Strait and ends some 700 km south of Singapore. It includes within its boundaries large shelf regions and deep basins. The major basin between the Philippines and Vietnam is around 4300 m deep; in its eastern part it contains numerous seamounts studded with coral reefs. To the east of this basin is a moderately wide shelf which narrows southwards to about 50 km along the coast of Vietnam between 12° - 15°S. Further south the shelf widens to one of the largest shelf areas of the world ocean, covering the region between eastern and western Malaysia and Indonesia west of 109°E and south of 5°N. By convention this shelf region, known as the Sunda Shelf, is included in the South China Sea, with the exception of the Gulf of Thailand which will be addressed in the next section.

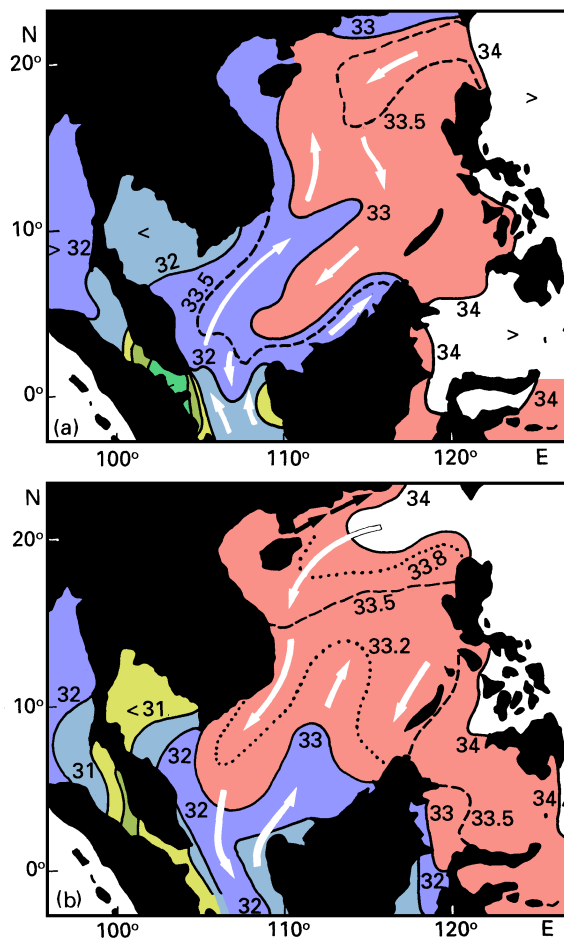


Fig. 10.14. Sea surface salinity in the South China Sea.

(a) During the southwest monsoon (August),

(b) during the northeast monsoon (February). Arrows indicate the inferred direction of flow.

After Wyrtki (1961).



throughout the year, fed by an offshoot from the Kuroshio. More recent observations have shown that this flow is interrupted by the northeast monsoon, which holds the warm tropical Kuroshio water back behind a front (Figure 10.15). The Kuroshio water then passes to the south of Taiwan and rejoins the main Kuroshio path. The front is broken during periods of weak winds, when large parcels of Kuroshio water manage to escape through Taiwan Strait into the East China Sea. There is thus still a net supply of water from the South China Sea during winter, but it occurs sporadically rather than continuously and is related to variations in the strength of the northeast monsoon.

### The Australasian shelf seas

The last group of marginal seas to consider are found in the regions to the west, and to the southeast, of the Australasian Mediterranean Sea. Both regions belong to continental shelves and thus cannot be discussed in detail without an understanding of coastal and shelf dynamics. We therefore conclude this chapter with a very brief summary of their features without going into much details of what brings those features about.

The seas to the west and northwest of the Australasian Mediterranean Sea form part of the largest shelf region of the world ocean, which consists of the Gulf of Thailand, the Sunda Shelf, Malacca Strait, and the Java Sea. With depths in the range 40 - 80 m this shelf is shallower than most shelves bordering the oceans.

The *Gulf of Thailand* has a bowl-shaped topography with average depth of 45.5 m and maximum depth of 83 m in the centre. It is separated from the South China Sea by a sill with 58 m sill depth and can be considered a large estuary or mini-mediterranean sea with negative  $E - P$  balance (see Chapter 7 for a discussion of mediterranean sea dynamics; precipitation  $P$  here includes river runoff). Its hydrography thus shows a two-layer system with low-salinity water leaving the Gulf near the surface and colder, more saline water entering near the bottom. Average surface salinities are in the range 31 - 32 throughout the year. The inflowing water has a temperature below 27°C and a salinity above 34. This water fills the Gulf below about 50 m depth. Currents are variable, responding to the seasonal cycle of the monsoon winds which are generally weak and variable over the Gulf. The weak mean flow is clockwise during summer, anti-clockwise during winter.

The Sunda Shelf forms part of the South China Sea; its circulation and hydrography was addressed in the last section. At 3°S it connects through Karimata Strait with the *Java Sea*, a shallow region with average depths around 40 - 50 m. The Java Sea was formed by the drowning of two large river systems which now form shallow channels in the otherwise flat sea floor. Its circulation and hydrography is determined by the monsoon winds, which in this region show the same annual cycle as the winds over the Australasian Mediterranean Sea (Chapter 13). Currents flow westward from June to August and eastward during the remaining eight months. A tongue of high salinity from the South China Sea (Figure 10.14b) then penetrates deep into the Java Sea, pushing the 32 isohaline as far east as 112°E.

To the south of the Sunda Island arch, the southern boundary of the Australasian Mediterranean Sea, is the extensive shelf of the Australian continent which embraces the Timor and Arafura Seas and the Gulf of Carpentaria. The *Timor Sea* between the island of Timor and northern Australia is characterized by a narrow trench on its northern side and a

